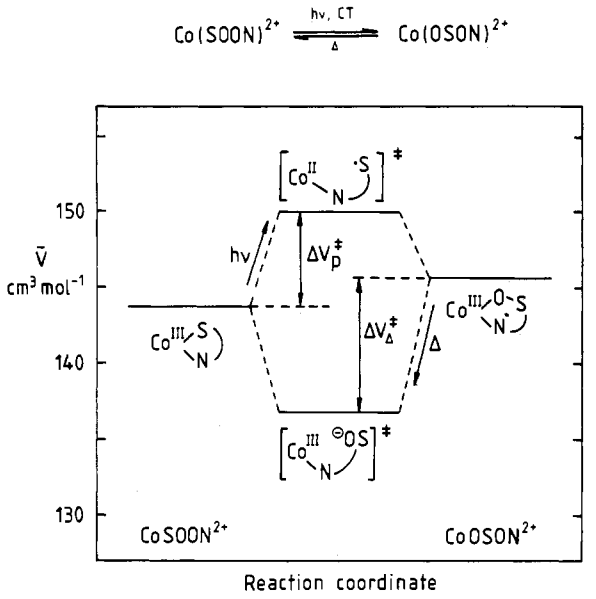

Figure 1. Reaction volume profile for the photochemical and reverse thermal isomerization of CoSOON. In this scheme it is assumed that $\bar{V}$(CoSOON*^{CT}) ~ $\bar{V}$(CoSOON) (see Discussion).

trans-$Cr(C_2O_4)_2(H_2O)_2^-$, for which a volume of activation of −16 ± 1 cm^3 mol^{-1} was found. In this case all the available evidence is consistent with a rate-determining opening of the oxalate ring,[23-25] and the large negative ΔV^* was ascribed to the increase in electrostriction around the negatively charged free end of the oxalate ligand.

We conclude that both the photochemical and thermal isomerization back-reactions occur via ring opening of the sulfinate ligand. No charge creation occurs in the case of the photochemical reaction such that the increase in volume of 6 cm^3 mol^{-1} should represent the pure intrinsic component. For the thermal reaction, ring opening accompanied by charge creation results in a volume decrease ca. 15 cm^3 mol^{-1} more negative, such that this quantity must present the change in volume due to electrostriction. In order to combine these data in an overall volume profile, the partial molar volume of $[Co(en)_2(SO_2CH_2CH_2NH_2)](ClO_4)_2$ was measured at 244.8 ± 1.8 cm^3 mol^{-1} from the apparent molar volume, which was independent of concentration over the range investigated. Taking into account that $\bar{V}(ClO_4^-)$ = 50.7 cm^3 mol^{-1},[10,11] it follows that $\bar{V}$(CoSOON) = 143.8 ± 1.8 cm^3 mol^{-1}. Density measurements on a sample of CoSOON irradiated almost to completion resulted in $\bar{V}$(CoOSON) = 145.7 ± 1.6 cm^3 mol^{-1}. The trend in the $\bar{V}$ data is in agreement with a slight increase in volume due to the formation of a six- instead of a five-membered ring complex. A combination of these $\bar{V}$ data and the reported volumes of activation enable the construction of the reaction volume profile given in Figure 1. It was assumed that the CT state has a partial molar volume close to that of the ground-state species as discussed above. If this is not the case, the transition state for the photochemical path will have an even higher partial molar volume, since the CT state can be up to 10 cm^3 mol^{-1} larger than the ground state (see earlier discussion). The profile clearly demonstrates the difference of at least 13 cm^3 mol^{-1} between the two transition states and the effect of electrostriction during the thermal back-reaction. To our knowledge this is the first example of a volume profile for a combined photochemical forward reaction and thermal back-reaction.

Acknowledgment. The authors gratefully acknowledge financial support from the Deutsche Forschungsgemeinschaft and the Fonds der Chemischen Industrie.

Registry No. $Co(en)_2(SO_2CH_2CH_2NH_2)^{2+}$, 75249-42-2; $Co(en)_2(OS(O)CH_2CH_2NH_2)^{2+}$, 75235-15-3.

(25) Kendall, P. L.; Lawrance, G. A.; Stranks, D. R. *Inorg. Chem.* **1978**, *17*, 1166.

Contribution from the Institut für Anorganische Chemie und Strukturchemie, Universität Düsseldorf, D-4000 Düsseldorf, Federal Republic of Germany

Fluorides and Fluoro Acids. 10.[1] Crystal Structures of Acid Hydrates and Oxonium Salts. 23.[2] Crystal Structure of the Low-Temperature Form of Oxonium Hexafluoroarsenate(V)

Dietrich Mootz* and Michael Wiebcke

Received January 30, 1986

Oxonium hexafluoroarsenate(V), H_3OAsF_6, is reported[3,4] to be cubic at room temperature, with disordered ions centered on the atomic positions of the NaCl structure, and to exist in a second, less symmetrical form below a transition point of 271 ± 5 K. The present paper deals with a complete X-ray single-crystal structure analysis of the low-temperature form.

Experimental Section

Preparation and Phase Analysis. H_3OAsF_6 was prepared as described[3] by reacting AsF_5 with HF and H_2O in a PTFE vacuum system. The AsF_5 was prepared by D. Naumann by reacting arsenic with a fluorine–nitrogen stream. The anhydrous HF was obtained by rectifying technical grade hydrofluoric acid (Riedel-de Häen, 71–75%) in a PTFE apparatus.

DTA and X-ray powder analysis between 103 and 303 K were applied to check the phase transition and high-temperature unit cell. The apparatus and techniques used are described and referred to elsewhere.[5]

Crystal Growth. A single crystal of the low-temperature form of H_3OAsF_6 was grown on a Syntex $P2_1$ four-circle diffractometer equipped with a modified low-temperature device. The starting material, a solution of H_3OAsF_6 in anhydrous HF, was sealed in polyethylene tubing (diameter 0.4 mm inside, 0.8 mm outside), which in turn for mechanical fixation was enclosed in a thin-walled glass capillary. A miniature zone-melting technique using focused heat radiation[6] was applied with the temperature of the cold gas stream at 243 K.

Structure Determination. The X-ray measurements for the structure determination were done on the diffractometer with the temperature of the crystal lowered to 208 K. The reflection intensities were not corrected for absorption because of an uncertain shape and size of the crystal within the tubing and angular restrictions for a ψ-scan with the low-temperature device used. The structure was solved from the Patterson function and refined in the space group $P\bar{1}$ by the method of full-matrix least squares minimizing the function $\sum w(|F_o| - |F_c|)^2$ with the weights $w = 1/(\sigma_F^2 + 0.0004F_o^2)$. The hydrogen atoms were located in a difference Fourier map of the electron density and included in the refinement. An isotropic extinction correction $F' = F_c/(1 + 0.002gF_c^2/\sin 2\theta)^{1/4}$ was applied and refined to g = 0.144 (6). More experimental and computational figures of the structure determination are assembled in Table I. Scattering factors of the neutral atoms with anomalous dispersion coefficients[7] were used in the SHELXTL[8] program system on a Data General Eclipse S/200 computer.

Since a statistical analysis of the normalized structure factor amplitudes had given some evidence for an acentric structure, in accordance with the IR and Raman spectra,[3,4] refinement in the space group $P1$ was also tried but not found preferable.

Results

Phase Transition. From the DTA and X-ray powder measurements the (reversible) phase transition to the high-temperature

(1) Part 9: ref 5.
(2) Part 22: Mootz, D.; Boenigk, D. *Z. Naturforsch., B: Anorg. Chem., Org. Chem.* **1984**, *39B*, 298.
(3) Christe, K. O.; Schack, C. J.; Wilson, R. D. *Inorg. Chem.* **1975**, *14*, 2224.
(4) Christe, K. O.; Charpin, P.; Soulie, E.; Bougon, R.; Fawcett, J.; Russel, D. R. *Inorg. Chem.* **1984**, *23*, 3756.
(5) Mootz, D.; Poll, W. *Z. Naturforsch., B: Anorg. Chem., Org. Chem.* **1984**, *39B*, 1300.
(6) Brodalla, D.; Mootz, D.; Boese, R.; Osswald, W. *J. Appl. Crystallogr.* **1985**, *18*, 316.
(7) Ibers, J. A., Hamilton, W. C., Eds. *International Tables for X-ray Crystallography*; Kynoch: Birmingham, England, 1974; Vol. IV.
(8) Sheldrick, G. M. *Structure Determination System - Reversion 4*; Nicolet: Cupertino, CA, 1983.

0020-1669/86/1325-3095$01.50/0

Table I. Crystal Data and Figures Related to Diffractometry and Refinement

cryst syst	triclinic
space group; Z	$P\bar{1}$; 2
a, Å	4.868 (3)
b, Å	6.471 (2)
c, Å	7.525 (4)
α, deg	86.52 (3)
β, deg	85.23 (4)
γ, deg	81.09 (4)
V, Å^3	233.1 (2)
temp, K	208
density (calcd), g·cm^{-1}	2.96
scan mode	variable ω scan
radiation	monochromatized Mo Kα
wavelength, Å	0.71073
μ(Mo Kα), cm^{-1}	73.3
range of 2θ, deg	3–75
indices collcd	$h,\pm k,\pm l$
no. of total reflcns	2678
no. of indep. reflcns: all/obsd ($I > 1.96\sigma_I$)	2427/2337
R (all/obsd)	0.032/0.031
R_w (all/obsd)	0.045/0.045

Table II. Fractional Atomic Coordinates and Isotropic[a] Thermal Parameters (Å^2)

atom	x	y	z	B
As	−0.44870 (3)	0.23414 (2)	0.24376 (2)	0.971 (8)
F(1)	−0.3253 (4)	0.4677 (2)	0.2628 (2)	2.02 (3)
F(2)	−0.1888 (3)	0.1084 (2)	0.3753 (2)	1.88 (3)
F(3)	−0.2127 (4)	0.1839 (3)	0.0592 (2)	2.01 (3)
F(4)	−0.5562 (4)	−0.0020 (2)	0.2248 (2)	2.12 (3)
F(5)	−0.6943 (4)	0.3580 (3)	0.1084 (2)	2.11 (3)
F(6)	−0.6687 (4)	0.2841 (3)	0.4290 (2)	2.17 (3)
O	0.0370 (4)	0.7287 (3)	0.2712 (2)	1.72 (3)
H(1)	−0.075 (10)	0.652 (7)	0.261 (5)	2.9 (8)
H(2)	−0.023 (9)	0.833 (7)	0.324 (5)	2.7 (8)
H(3)	0.112 (13)	0.756 (8)	0.158 (6)	5.3 (12)

[a] For the non-hydrogen atoms calculated from the anisotropic B_{ij} by $^1/_3(B_{11}a^{*2}a^2 + \ldots + B_{23}b^*c^*bc\cos\alpha)$.

form was determined to occur at 275 K. This temperature and the powder patterns obtained for both phases are in good agreement with those of the previous work.[3,4]

Crystal Structure. The low-temperature form of H_3OAsF_6 crystallizes with the triclinic centrosymmetric space group $P\bar{1}$ and $Z = 2$ formula units per unit cell. The crystallographic data are given in Table I, and the atomic parameters in Table II. All atoms are ordered and are in general positions. Interatomic distances and angles are listed in Table III. The values are not corrected for thermal motion and the well-known systematic error of X-ray analysis to produce O–H bond lengths that are shorter than the internuclear distances.

The H_3O^+ cation has distorted trigonal-pyramidal geometry, and the AsF_6^- anion distorted octahedral geometry. Cations and anions are linked by three independent O–H···F hydrogen bonds to fluorine atoms F(1)–F(3) into parallel polymeric ribbons [010]. This is shown in Figure 1.[9] The ribbons are made up of fused centrosymmetric rings with two cations and two anions each and two alternating conformations.

The fluorine atoms F(4)–F(6) are not involved in hydrogen bonds. They have distinctly shorter As–F bonds than the atoms F(1)–F(3), to which they are in trans positions, and form in pairs the three largest of the *cis*-F–As–F bond angles. The shortest O···F and H···F approaches of atoms F(4)–F(6) are at 2.768 and 2.45 Å, respectively.

Discussion

A low site symmetry of the anion in the crystal structure (at most 3-C_3) was already inferred from the IR and Raman spectra.[3,4]

(9) Johnson, C. K. *Oak Ridge Natl. Lab. [Rep.] ORNL-5138*, 1976.

Table III. Interatomic Distances[a] (Å) and Angles[b] (deg)

Cation

O–H(1)	0.81	H(1)–O–H(2)	115
O–H(2)	0.81	H(1)–O–H(3)	106
O–H(3)	0.91	H(2)–O–H(3)	114

Hydrogen Bonds

	O···F	H···F	O–H···F
O–H(1)···F(1)	2.630	1.83	169
O–H(2)···F(2)[c]	2.667	1.89	160
O–H(3)···F(3)[d]	2.619	1.71	177

Anion

As–F(1)	1.729	As–F(2)	1.742	As–F(3)	1.740
As–F(4)	1.708	As–F(5)	1.707	As–F(6)	1.701

F(1)–As–F(2)	89.2	F(1)–As–F(3)	89.0
F(1)–As–F(4)	177.5	F(1)–As–F(5)	90.2
F(1)–As–F(6)	89.8	F(2)–As–F(3)	87.5
F(2)–As–F(4)	88.8	F(2)–As–F(5)	177.9
F(2)–As–F(6)	90.6	F(3)–As–F(4)	89.5
F(3)–As–F(5)	90.5	F(3)–As–F(6)	177.1
F(4)–As–F(5)	91.8	F(4)–As–F(6)	91.7
F(5)–As–F(6)	91.4		

[a] Esd's: 0.002 Å for As–F, 0.003 Å for O···F, 0.04–0.05 Å for H···F and O–H. [b] Esd's: 0.1° for F–As–F, 4–5° for H–O–H and O–H···F. [c] x, $1 + y$, z. [d] $-x$, $1 - y$, $-z$.

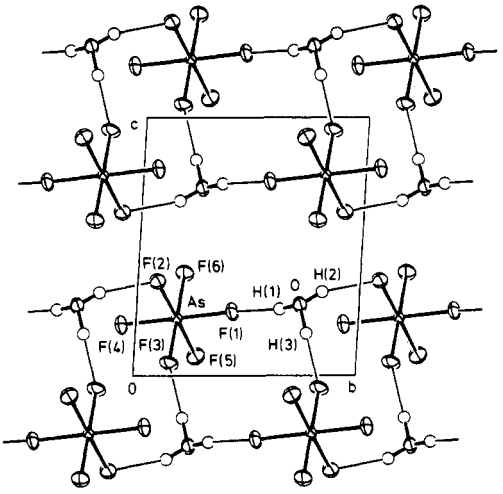

Figure 1. Projection on the b,c plane with 50% probability ellipsoids.

The observed lengthening of the bonds between the central atom and those fluorine atoms that are involved in hydrogen bonds is similar to that in oxonium salts of some other fluoro acids, e.g. H_3OBF_4,[10] H_3OTiF_5,[11] and D_3OSbF_6.[4] The hydrogen bonding distances O···F are somewhat longer than in these structures. None of the other interionic distances is smaller than the sum of the van der Waals radii of the respective atoms.

In spite of the different structures of the anions the crystal structure of the low-temperature form of H_3OAsF_6 is strikingly similar to that of H_3OBF_4.[10] This is true not only for the scheme of hydrogen bonding between the cations and anions but also with new axes $-a$, c, b for the crystallographic data and many of the atomic coordinates.

A shift of the origin to $^1/_2$, $^1/_4$, $^1/_4$ followed by another transformation of the axes according to $-a$, $(b + c)/2$, $(b - c)/2$ shows that the structure with its arrangement of the oxygen and arsenic atoms of the cations and anions, respectively, is a distorted variant of the CsCl structure type. This is in contrast to the high-temperature form of H_3OAsF_6, which by disorder is highly symmetrical and a representative of the NaCl structure type.[3,4]

Two related salts with a substituted cation and anion, respectively, also have ordered, but not isotypic, CsCl-like structures

(10) Mootz, D.; Steffen, M. *Z. Anorg. Allg. Chem.* **1981**, *482*, 193.
(11) Cohen, S.; Selig, H.; Gut, R. *J. Fluorine Chem.* **1982**, *20*, 349.

Table IV. X-ray Diffraction Powder Pattern of H_3OSbF_6 at about 370 K[a]

d_{obsd}, Å	d_{calcd}, Å	intens	*hkl*
5.12	5.12	vs	100
3.62	3.62	s	110
2.957	2.960	vw	111
2.560	2.563	w	200
2.293	2.292	vw	210
2.096	2.093	vw	211
1.813	1.813	vw	220
1.711	1.709	w	300, 221
1.621	1.621	w	310
1.371	1.370	w	321
1.281	1.282	vw	400
1.242	1.243	vw	410, 322
1.209	1.208	vw	411, 330

[a] Cubic, a = 5.126 (1) Å, V = 134.7 (1) Å^3, Z = 1, ρ_{calcd} = 3.14 g cm^{-3}, monochromatized Cu Kα_1 radiation (λ = 1.540 562 Å), Guinier-Simon camera, diameter 114.6 mm.

at low temperatures: $KAsF_6$ with one formula unit in a rhombohedral cell[12] and H_3OSbF_6 (as well as D_3OSbF_6) with eight formula units in a cubic, but large, body-centered cell.[4] In comparison, the high-temperature form of $KAsF_6$[13] is isotypic to that of H_3OAsF_6. For the structure of a high-temperature form of H_3OSbF_6 see the Appendix.

Acknowledgment. We are grateful to Prof. D. Naumann, Universität Dortmund, for providing the AsF_5. The work was supported by the Minister für Wissenschaft und Forschung des Landes Nordrhein-Westfalen and by the Fonds der Chemischen Industrie.

Appendix: Unit Cell of H_3OSbF_6 at about 370 K

H_3OSbF_6 was prepared and studied by DTA and X-ray powder analysis between 103 and 423 K in a similar way as described in the Experimental Section for H_3OAsF_6. The phase transition in this temperature range, reported to occur at 361 ± 12 K,[4] was found at 368 K. Also, the reported X-ray powder pattern and crystal structure of the low-temperature form[4] was confirmed. In addition, the powder pattern of the high-temperature form was obtained and indexed for a cubic primitive unit cell with Z = 1 and a = 5.126 (1) Å (Table IV). From this the ions appear to be centered on the atomic positions of the small unit cell of the CsCl structure type.

Registry No. H_3OAsF_6, 21501-81-5; H_3OSbF_6, 55649-03-1.

Supplementary Material Available: A listing of anisotropic thermal parameters (1 page). Ordering information is given on any current masthead page.

(12) Gafner, G.; Kruger, G. J. *Acta Crystallogr., Sect. B: Struct. Crystallogr. Cryst. Chem.* **1974**, *B30*, 250.
(13) Heyns, A. M.; Pistorius, C. W. F. T. *Spectrochim. Acta, Part A* **1975**, *31A*, 1293.

Contribution from the Department of Chemistry, University of Western Ontario, London, Ontario, Canada N6A 5B7

Binuclear Complexes of Platinum(II) and Palladium(II) with Bis(isopropylphosphino)methane and Related Ligands

Wanda Radecka-Paryzek,*[1] Alistair J. McLennan, and Richard J. Puddephatt*

Received October 29, 1985

Bidentate phosphines $R_2PCH_2PR_2$ are often used as bridging ligands and are useful for reducing the tendency toward fragmentation of dimers to monomeric complexes during chemical reactions.[2,3] The chemistry of the secondary phosphine analogues such as R_2PCH_2PHR or $RHPCH_2PHR$ has hardly been studied.[4,5] through the presence of the PH group could lead to significantly different reactivity. Thus both the low steric hindrance of the PH substituent[6,7] and the ability of the PH group to undergo deprotonation and form a second potential bridging group, based on the resultant phosphido functionality,[8] could have major effects on the coordination chemistry. Earlier papers have been concerned with the effects of steric hindrance of ligands $R_2PCH_2PR_2$ on the coordination chemistry and organometallic reactivity of platinum complexes.[3,6,7,9] In this paper, the synthesis and some coordination complexes of the ligand *i*-PrHPCH$_2$PH-*i*-Pr are described.

Results and Discussion

Synthesis and Characterization of the Ligand. The ligand *i*-PrHPCH$_2$PH-*i*-Pr was prepared by reaction of $Cl_2PCH_2PCl_2$ with 2 molar equiv of *i*-PrMgBr followed by reduction of this reaction mixture with excess Li[AlH$_4$]. Analysis of the crude product by $^{31}P\{^1H\}$ and ^{31}P NMR indicated the presence of $H_2PCH_2PH_2$, *i*-PrHPCH$_2$PH$_2$ and *i*-Pr$_2$PCH$_2$PH-*i*-Pr as well as the desired compound. However, vacuum distillation gave a good separation of pure *i*-PrHPCH$_2$PH-*i*-Pr as a colorless, air-sensitive liquid. An independent synthesis of the ligand was reported while this research was in progress.[5] The ligand exists either as a mixture of isomers or in a configuration in which the two phosphorus atoms are nonequivalent but do not couple to each other, as shown by the $^{31}P\{^1H\}$ NMR spectrum, which contained two sharp singlets, of approximately equal intensity, at δ −46.20 and −47.61, each of which split into a doublet [^1J(PH) = 205 Hz] in the proton-coupled ^{31}P spectrum. Similarly, the ^1H NMR spectrum contained two C*H*Me$_2$ and two CH_2P$_2$ multiplets, tentatively attributed to the two isomeric forms, though the P*H* and CH_3C resonances of the two isomers were not resolved. The two isomers could be the racemic and meso isomers I and II, but it is also possible that they

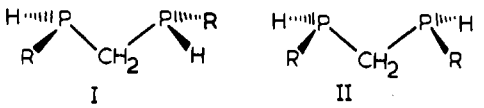

are conformers that cannot readily interconvert due to restricted rotation about the P–C bonds.

Synthesis and Characterization of $[M_2X_4(\mu\text{-PP})_2]$ Complexes. Reaction of $[PtCl_2(SMe_2)_2]$ with PP in a 1:1 molar ratio gave the binuclear *cis,cis*-$[Pt_2Cl_4(\mu\text{-PP})_2]$ in two isomeric forms, **1a** and **1b**, which were easily separated by taking advantage of the much greater solubility of **1b** in organic solvents. Isomer **1a** gave a singlet, with apparent doublet satellites due to coupling to ^{195}Pt [^1J(PtP) = 3360, ^3J(PtP) = 80, $^2J + {}^4J$(PP) = 36 Hz], characteristic of the cis,cis stereochemistry with phosphorus trans to Cl.[7] These data are very similar to those for *cis,cis*-[Pt$_2$Cl$_4$(μ-*t*-BuHPCH$_2$PH-*t*-Bu)$_2$], and **1a** therefore has the symmetrical structure III with M = Pt, X = Cl, and R = *i*-Pr, in which all bulky isopropyl groups are equatorial and in which both diphosphine ligands are in the racemic form (I).

In contrast, the isomer **1b** gave four multiplets of equal intensity in the $^{31}P\{^1H\}$ NMR spectrum, each with ^1J(PtP) = 3300–3360

(1) On leave from Department of Chemistry, A. Mickiewicz University, Poznan, Poland.
(2) Balch, A. L. In *Homogeneous Catalysis with Metal Phosphine Complexes*; Pignolet, L., Ed.; Plenum: New York, 1983.
(3) Puddephatt, R. J. *Chem. Soc. Rev.* **1983**, 99.
(4) Brauer, D. J.; Hietkamp, S.; Sommer, H.; Stelzer, O. *Angew. Chem., Int. Ed. Engl.* **1984**, *23*, 734.
(5) Hietkamp, S.; Sommer, H.; Stelzer, O. *Chem. Ber.* **1984**, *117*, 3400.
(6) Steric effects on the chemistry of $R_2PCH_2PR_2$ ligands have been discussed previously: (a) Manojlović-Muir, Lj.; Muir, K. W.; Frew, A. A.; Ling, S. S. M.; Thomson, M. A.; Puddephatt, R. J. *Organometallics* **1984**, *3*, 1637. (b) McLennan, A. J.; Puddephatt, R. J. *Organometallics* **1985**, *4*, 485. (c) Kullberg, M. L.; Kubiak, C. P. *Organometallics* **1984**, *3*, 632. (d) Lee, K.-W.; Brown, T. L. *Organometallics* **1985**, *4*, 1025.
(7) Azam, K. A.; Ferguson, G.; Ling, S. S. M.; Parvez, M.; Puddephatt, R. J.; Srokowski, D. *Inorg. Chem.* **1985**, *24*, 2799.
(8) Chen, L.; Kountz, D. J.; Meek, D. W. *Organometallics* **1985**, *4*, 598.
(9) Manojlović-Muir, Lj.; Jobe, I. R.; Ling, S. S. M.; McLennan, A. J.; Puddephatta, R. J. *J. Chem. Soc., Chem. Commun.* **1985**, 1725.

0020-1669/86/1325-3097$01.50/0